International Journal of Pharmaceutics 606 (2021) 120868

Contents lists available at ScienceDirect

International Journal of Pharmaceutics

journal homepage: www.elsevier.com/locate/ijpharm

Enhanced skin retention and permeation of a novel peptide via structural modification, chemical enhancement, and microneedles

Jungen Chen [a,b,1], Junxing Bian [a,1], Basil M. Hantash [c], Lamyaa Albakr [d], David E. Hibbs [a], Xiaoqiang Xiang [e], Peng Xie [e,f], Chunyong Wu [b,*], Lifeng Kang [a,*]

[a] School of Pharmacy, Faculty of Medicine and Health, University of Sydney, Sydney, NSW 2006, Australia
[b] Department of Pharmaceutical Analysis, China Pharmaceutical University, Nanjing, JS 210009, China
[c] Escape Therapeutics Inc., 3800 Geer Road, Suite 200, Turlock, CA 95382, USA
[d] Department of Pharmaceutics, King Saud University, 11454 Riyadh, Saudi Arabia
[e] School of Pharmacy, Fudan University, Shanghai 201203, China
[f] China State Institute of Pharmaceutical Industry, Shanghai 201203, China

ARTICLE INFO

Keywords:
Peptide
Hyperpigmentation
Transdermal
Prodrug
Enhancers
Microneedles

ABSTRACT

Hyperpigmentation is a common skin condition with serious psychosocial consequences. Decapeptide-12, a novel peptide, has been found to be safer than hydroquinone in reducing melanin content, with efficacy up to more than 50% upon 16 weeks of twice-daily treatment. However, the peptide suffers from limited transcutaneous penetration due to its hydrophilicity and high molecular weight. Therefore, decapeptide-12 was modified by adding a palmitate chain in an attempt to overcome this limitation. Molecular docking results showed that the two peptides exhibited similar biological activity towards tyrosinase. We also tested the effect of chemical penetration enhancers and microneedles to deliver the two peptides into and through skin, using an *in vitro* human skin permeation method. It was shown that the palm-peptide achieved the best skin retention owing to the increased lipophilicity. In addition, skin permeation of the palm-peptides was enhanced by the chemical skin penetration enhancers, namely, oleic acid and menthol. Skin permeation of the native peptide was enhanced by the microneedle patch but not the chemical skin penetration enhancers. Cutaneous absorption of the palm-peptides was estimated to have achieved its therapeutic concentration within skin. The combinatory approach of using molecular modification, chemical penetration enhancement, and microneedle patch proves to be useful to enhanceskin permeation of the peptides.

1. Introduction

Melanin, the end product of melanogenesis, plays a crucial role in the absorption of free radicals generated within the cytoplasm, shielding the host from various types of ionizing radiations, and determining the color of human skin, hair, and eyes (Parvez et al., 2006). However, excess production of melanin can cause skin hyperpigmentation, a common and non-life-threatening disorder. Melasma is a form of hyperpigmentation that causes brown or gray patches on the skin, primarily in the facial area. Hydroquinone and tretinoin, combined with topical corticosteroids, are well established therapeutic agents for melasma and hyperpigmentation (Torok, 2006).

Recently, Hantash and his group reported that a novel proprietary synthetic peptide, namely, decapeptide-12 (the native peptide, Fig. 1a), demonstrated a stronger competitive inhibition effect on mushroom and human tyrosinase enzymes than hydroquinone (Abu Ubeid et al., 2009). Additional studies on humans demonstrated the therapeutic effect of Lumixyl™, a topical formulation containing decapeptide-12, for the treatment of melasma (Hantash and Jimenez, 2009, 2012). Nonetheless, the topical formulation contains excipients which may cause side effects, such as skin barrier disruption and skin irritation, posinga major obstacle for further product development. This has motivated us to carry

* Corresponding authors at: Key Laboratory of Drug Quality Control and Pharmacovigilance, Ministry of Education, China Pharmaceutical University, No 24 Tongjia Road, Nanjing, China. (C. Wu). School of Pharmacy, Faculty of Medicine and Health, Pharmacy and Bank Building A15, Science Road, University of Sydney, Sydney, NSW 2006, Australia (L. Kang).
E-mail addresses: cywu@cpu.edu.cn (C. Wu), lifeng.kang@sydney.edu.au (L. Kang).
[1] These authors contributed equally to this work.

https://doi.org/10.1016/j.ijpharm.2021.120868
Received 23 February 2021; Received in revised form 14 June 2021; Accepted 3 July 2021
Available online 6 July 2021

out further investigations to enhance skin permeation and retention of the peptide, a relatively large hydrophilic molecule containing 10 amino acids. The effective skin permeation of the peptide is important to maintain its therapeutic concentration inside skin, where both melanocytes and melanocyte progenitors reside (Cichorek et al., 2013).

While decapeptide-12 could reduce melanin's production (Abu Ubeid et al., 2009), its skin permeation profile remains unclear. As shown in Fig. 1a, decapeptide-12 is a polar molecule with multiple amino and hydroxyl groups which can hinder transdermal absorption through the lipophilic stratum corneum (SC) (Kumar and Philip, 2007). To enhance the skin permeation of the peptide, multiple options are available, e.g., molecular modification (Lim et al., 2018), using chemical penetration enhancers (CPEs) (Kang et al., 2007), or microneedles (MNs) (Lim et al., 2020).

For molecular modification, many studies have focused on improving the biostability and bioavailability of peptides for oral, pulmonary, and nasal administration (Antosova et al., 2009). Due to the lipophilic nature of the SC barrier, peptides existing in zwitterionic form can only permeate minimally through skin. To this end, molecular modification of peptide by increasing its lipophilicity may enhance its skin permeation. In a previous study, we have shown that enhanced skin permeation can be achieved by modifying the structure of a hexapeptide to make it more lipophilic (Lim et al., 2018). In this study, we palmitoylated the peptide to form a new peptide molecule (the palm-peptide, Fig. 1b), to increase its lipophilicity. Both peptides comprise a phenol group at their C-terminals, which can potentially serve as a substrate to compete with phenols such as tyrosine (Fig. 1c), in docking with tyrosinase to inhibit melanogenesis. To ensure that the molecular modification will not compromise its biological activity as a tyrosinase inhibitor, a molecular docking study was performed.

On the other hand, chemicals can interact with the intercellular lipids inside the SC to enhance drug permeation through skin (Kang et al., 2006). Many CPEs, such as fatty acids and terpenes, play an essential role in promoting drug permeation through the skin (Ahad et al., 2009). Propylene glycol (PG) is a common cosmetic vehicle and shows synergistic action when being used together with other CPEs (Williams and Barry, 2012). It has been shown that PG can solubilize the SC intercellular lipids (Kang et al., 2006). In addition, PG has no alcoholic smell, which could help to improve patient compliance. In this study, oleic acid, camphor, and menthol, all of which are widely used CPEs (Morimoto et al., 2002; Pierre et al., 2006; Xie et al., 2016), were selected as candidate CPEs.

In addition to chemical enhancement, physical methods such as electroporation, iontophoresis, diamond microdermabrasion, laser radiation, and ultrasound may also increase transcutaenous penetration (Bhatia et al., 2014; Costello and Jeske, 1995; Gómez et al., 2012; Hantash, 2018; Lombry et al., 2000; Mitragotri et al., 1995). But disadvantages such as high costs have limited their applications. Recently, MNs (Ma and Wu, 2017) have emerged as a powerful tool to enhance the skin permeation of a variety of biomolecules, including oligonucleotides, peptides, proteins, and vaccines (Prausnitz, 2004). MNs can be applied onto skin surfaces to create an array of microscopic passages through which the biomolecules can reach the dermis (Schuetz et al., 2005). Previously, we reported the application of microneedles on transdermal delivery of lidocaine (Kathuria et al., 2016), copper-peptide (Li et al., 2015), and nucleic acids (Koh et al., 2018). Here, menthol was investigated as a novel material to fabricate MN patches by micromolding. Menthol has a low melting point close to human body temperature (Kang et al., 2007), which is useful for its dissolution upon contact with skin. Hence, menthol has dual functions, i.e., acting as a CPE and a physical penetration enhancer.

In this study, we investigated decapeptide-12 and its analogue with higher lipophilicity, on their ability to permeate skin using both CPEs and MNs. We hypothesized that the increased lipophilicity can increase its skin permeation. Apart from molecular modification, chemical and physical enhancements were also investigated. The aim was to find an effective approach by using the three methods (molecular modification, CPE, MN, or any combination of the three methods) to enhance skin

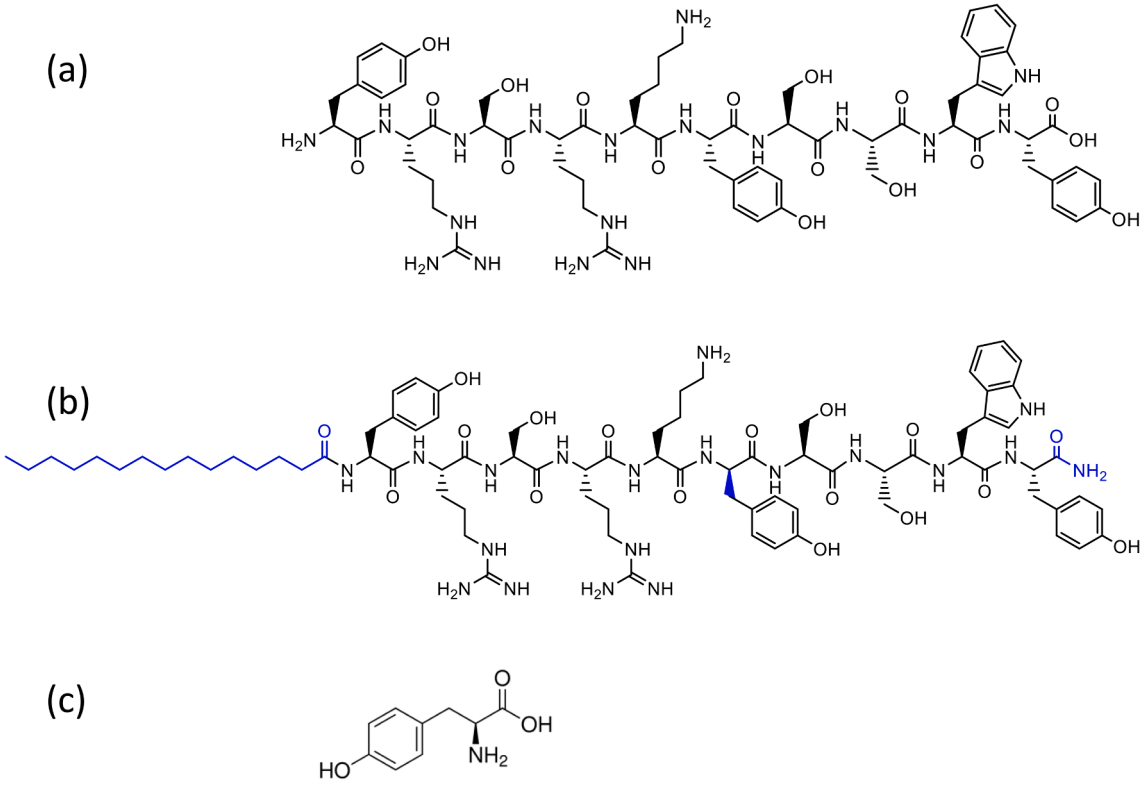

Fig. 1. Molecular structures of the native peptide (**a**), palm-peptide (**b**), and tyrosine (**c**). For palm-peptide, N-terminal was palmitoylated, C-terminal was modified to amide, and tyrosine at position 6 changed from *L*- to *D*- form.

permeation of the peptide. The efficacy of different peptide delivery systems was determined with *in vitro* permeation test (IVPT), using human dermatomed cadaveric skin samples.

2. Methods

2.1. Materials

The native peptide and palm-peptide were synthesized by Bio Basic Inc. (Ontario, Canada). The PG and phosphate-buffered saline (PBS) tablets were purchased from VWR, USA. The oleic acid, penicillin–streptomycin, and trifluoroacetic acid were purchased from Sigma-Aldrich, USA. Camphor powder was purchased from New Directions, Australia. The (-)-menthol crystals were purchased from WFmed, USA. Phosphoric acid solution (85 wt% in water) was purchased from Sigma-Aldrich, USA. Acetonitrile was obtained from RCI Labscan, Thailand. Methanol was obtained from Honeywell, USA. The human epidermis was provided by Science Care, USA. All materials were used as supplied without further purification.

2.2. Preparation of tyrosinase structure

The crystal structure of tyrosinase from *Bacillus megaterium* (Protein Data Bank (PDB) code: 4P6T) was imported into the Schrödinger software (Release 2020). The protein structure was prepared with the Protein Preparation Tool. The asparagine (Asn), glutamine (Gln) and histidine (His) residues were automatically checked for protonated states. The hydrogen atoms were added into the structures at the physiological pH environment, using the PROPKA tool in Maestro of the Schrödinger software with an optimized hydrogen-bond network.

2.3. Molecular docking

The geometry of native peptide and the palm-peptide were built in the Discovery Studio 3.5 and saved in sdf file format, respectively. The resultant structures of peptides were imported in Maestro and subjected to a Monte Carlo Multiple Minimum conformational search, using the MMFFs force field. The docking pocket Grid file of tyrosinase was generated by 36 Å around the substrates in the active site with the Receptor Grid Generation module and docked with Glide Docking module. The Van der Waals scaling was set to 0.8 for nonpolar atoms of receptor and ligand. During docking, the number of docking output was set as 100 poses per docking run.

2.4. Peptide synthesis and characterization

The native peptide and its analogue palm-peptide were synthesized by Bio Basic Inc., using fluorenyl methyl oxycarbonyl chloride (FMOC) based synthetic method on Rink-amide resin with modifications specific to each compound (Fig. 2). The side-chain protecting groups used were: Tyrosine(*tert*-butyl tBu), Tryptophan (*tert*-butyloxycarbonyl, Boc), Serine (tBu), Lysine (Boc), and Arginine (2,2,4,6,7-pentamethyldihydrobenzofuran-5-sulfonyl, Pbf). Synthesis was performed using FMOC-Tyrosine (tBu)-2-Chlorotrityl resin for native peptide, and Rink amide Aminomethyl (AM) resin for palm-peptide, respectively.

An initial deprotection of bubbling nitrogen through dimethylformamide (DMF) containing 20% piperidine was followed by a 5-min wash in DMF five times. Conjugation reaction was performed in 500 mL DMF containing 19.3 g 2-(1H-benzotriazole-1-yl)-1,1,3,3-tetramethylaminium tetrafluoroborate (TBTU) and 18.6 mL N,N-diisopropylethylamine (DIEA). The product was washed three times using DMF after drying. The whole process was repeated until the conjugation of all the protected amino acids was complete. After the conjugation reaction, the on-resin peptide was washed with methanol, dichloromethane, and methyl alcohol, sequentially. Drying and lyophilizing process were then carried out.

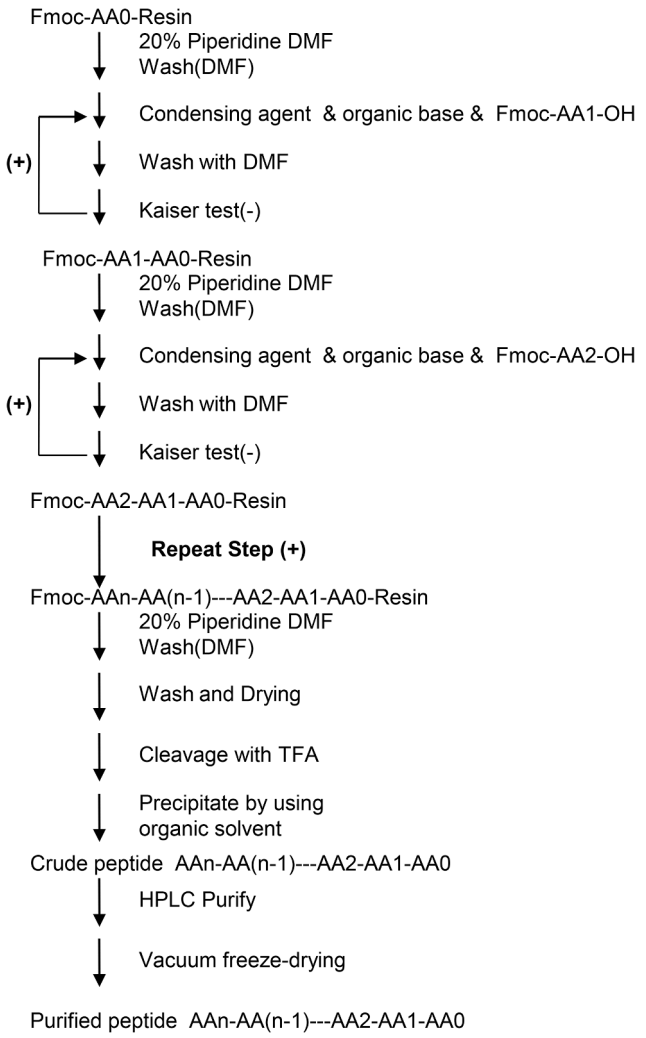

Fig. 2. The flow chart of peptide synthesis process.

The cleavage was performed using 1000 mL of reagent (82.5% trifluoroacetic acid (TFA) + 5% 1,2-ethanedithiol + 5% water + 5% p-cresol + 2.5% thioanisole) for 2 h. Afterwards, the resin particles were filtered using a sand-core funnel, for the coarse product to precipitate in the filtered liquid.

The crude peptide was purified using a reversed phase high performance liquid chromatography (HPLC) method, using a Kromasil C18 column (250 × 4.6 mm, 5 μm). The mobile phase consisted of mobile phase A (acetonitrile) and mobile phase B (0.1% v/v trifluoroacetic acid in water). A gradient elution program was used with the ratio of phase A and phase B as follows: 76 – 56% B for 0–120 min. The flow rate was set at 1 mL/min. The ultraviolet detection wavelength was set at 220 nm. The sample with a purity higher than 80% was collected, then concentrated with a temperature around 35-40 °C. Following purification, the peptide solution was lyophilized for 24 h, at -40 °C.

2.5. Peptide physicochemical properties

In silico prediction of physicochemical properties of two peptides was performed using the Qikprop v6.2 package, which is part of the Schrödinger software (Release 2020).

2.6. Saturated peptide solution preparation

Peptide solubility was determined in PG to prepare saturated peptide solutions. Excess peptide was added into each solvent inside a 2 mL

Eppendorf tube which was kept shaking in an incubation orbital shaker (OM15C, Ratek, Australia) for 48 h. The set up was kept at room temperature. Samples were then centrifuged at 12,000 rpm for 10 min. Subsequently, the supernatant was transferred into an amber bottle for assay.

2.7. Fabrication of micromold

Using a previously reported method (Kathuria et al., 2020), the molds were fabricated via thermal curing of polydimethylsiloxane (PDMS), using the 3M Microchannel Skin System (3M Technologies, Singapore) as the master template. Briefly, the elastomer and curing agent were mixed and vacuumed at 95 kPa for 10–20 min to remove the entrapped air bubbles. Then, the mixture was poured slowly into the plastic petri dish for curing in an oven at 70 °C for 2 h. The cured PDMS was gently taken out from the petri dish using a surgical blade. The MN master was gently peeled off from the cured PDMS to get the PDMS mold.

2.8. Fabrication of MN patches bearing the peptides

PDMS molds were heated on a hot plate at 65 °C for approximately 10 min. While heating the PDMS molds, menthol was melted in a cuvette at 65 °C using a heating block (Major Science, USA). Peptide was then added into menthol and mixed well. PDMS molds were then removed from the hot plate, and the liquid mixture of menthol and peptide was poured into the mold. Afterwards, the PDMS mold containing the liquid mixture was kept at room temperature for the liquid mixture to solidify. Subsequently the MN patch was de-molded upon solidification.

2.9. Human skin membrane preparation

Human dermatomed skin was obtained from Science Care (Arizona, USA). The skin tissues were excised from the thighs of two male cadavers with age at death of 66 and 57. The skin samples were without identifier and exempted from ethical review. The integrity of cadaver skin was checked using visual inspection before use to ensure no pores or breaks in the skin surface were present. In addition, any compromise in skin integrity was identified through observation of a rapid and large increase in the amount of permeated peptide through the skin at the first sampling time point.

2.10. In vitro permeation test (IVPT)

Franz type static diffusion cells were used for the IVPT. The dermatomed human skin sample was mounted between donor and receptor compartments, with excessive skin at the sides being trimmed off to minimize lateral diffusion. The SC side was faced towards the donor compartment, with a permeation area of 1.327 cm^2. The receptor compartment was filled with 5.5 mL of 1 mM PBS containing 1% (v/v) penicillin/streptomycin (Invitrogen, USA). The receptor solution was filtered twice, using a membrane filter (pore size = 0.2 μm, Sigma-Aldrich, USA), to prevent the formation of air bubbles beneath the skin membrane during IVPT.

In total, 8 PG-based liquid formulations were tested, with 4 formulations containing native peptide and the other 4 containing palm-peptide. The concentration of CPEs in the solution was 5% w/v oleic acid, 5% w/v menthol, and 5% w/v camphor, respectively. The concentration of the peptide in each formulation is tabulated in the supplementary information (SI) **Tab. SI1**. The saturated concentration of native peptide in the PG solution was found to be ~ 200 mg/ml, based on our testing results. On the other hand, the saturated concentration of the palm-peptide was found to be <100 mg/ml in PG. As a result, the concentration of the native peptide was prepared 100 mg/ml, to be close to the saturated concentration of the solution containing the palm-peptide, as shown in **Tab. SI1.** For each liquid formulation, 250 μL ofsolution was added to the donor compartment and covered with wraps.

For the MN patches, 2 formulations were prepared, with one formulation containing native peptide and the other containing palm-peptide. The weight of each MN patch was ~ 100 mg, containing ~ 2 mg peptides (**Tab SI2**). The MN patch was first cut into a suitable size and weighed prior topermeation testing. Patches were then applied to the skin using a finger-thumb grip for 20 s. Scotch tape was used to fix the patches onto the skin. Triplicates were prepared for each formulation. The donor compartment and the sampling port were covered with wraps to minimize contamination and evaporation. Magnetic stirrers were set at 180 rpm to mix the receptor solution during the 24 h study. The device was kept at 32 °C, inside an incubator. 500 μL of the receptor fluid were collected at different time points for HPLC analysis and replaced with 500 μL of fresh receptor solution. The skin permeation study was conducted in a time course of 24 h.

2.11. HPLC method for the peptide analysis

The amount of peptide permeated was determined using a Shimadzu CBM-20A HPLC system with Agilent C18 column (4.6 mm × 250 mm, 5 μm, 170 Å). The mobile phase consisted of mobile phase A (0.1% v/v trifluoroacetic acid in water) and mobile B (0.1% v/v trifluoroacetic acid in acetonitrile) with a gradient elution program with ratios of solvents A and B as follows: native peptide (15 – 35% B for 0–20 min and 15% for 20.01–30 min), palm-peptide (45 – 55% B for 0–10 min and 55% for 10.01–30 min) The flow rate was 1.0 mL/min. The injection volume was 50 μL, and ultraviolet detection was performed at 280 nm. A calibration curve was established using the standard solutions from 5 μg/mL to 50 μg/mL for native peptide and from 1 μg/mL to 50 μg/mL for palm-peptide.

The amount of peptide retained inside the skin sample was analyzed following the procedure below. Upon completion of the skin permeation experiment at 24 h, the skin sample was removed from the Franz cell. The surface of the skin sample was wiped with cotton swaps soaked in 75% (v/v) ethanol, to remove any residual peptide on the skin surface. Afterwards, the cleaned skin sample was cut into small pieces, ground into a homogenate using 2 mL PBS, transferred to a centrifuge tube, and shaken overnight at 37 °C, in a shaking incubator. The homogenate was centrifuged at 10,000 rpm for 10 min to precipitate the skin tissue. Then the supernatant was taken out, filtered through a syringe filter with a 0.45 μm membrane, and analyzed with the HPLC method.

2.12. Statistical analysis

All data were collated and prepared using GraphPad Prism 8 (GraphPad Software Inc, CA, USA). Results were expressed as mean ± standard deviation of at least three independent experiments. Statistical analysis was performed by one-way analysis of variance (ANOVA). The difference was statistically significant at p-value < 0.05.

3. Results

3.1. Docking of the peptides with tyrosinase

Tyrosinase is a di-copper oxidase, responsible for the production of the pigment melanin in many organisms. Its molecular structure comprises six histidine residues that coordinate the two copper ions, namely, CuA and CuB, which form the active site of tyrosinase. The crystal structure of tyrosinase with L-tyrosine has been previously reported (Goldfeder et al., 2014). In the docking study of L-tyrosine into the active site of tyrosinase, it was shown that the phenolic group of tyrosine was directed towards a zinc ion (at the equivalent position of CuA) at a distance of 1.9 Å, while the benzyl ring of L-tyrosine was oriented through hydrophobic π–π interactions with the histidine residue of H208 (Fig. 3a) (Goldfeder et al., 2014).

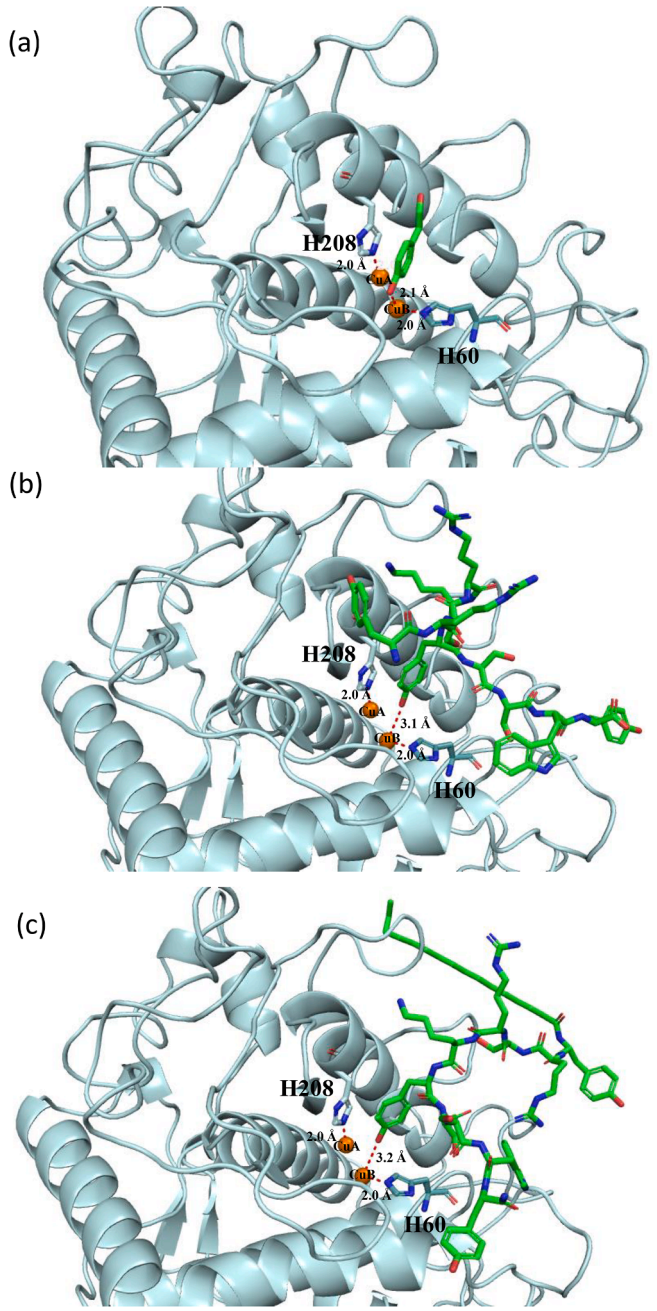

Fig. 3. The crystal structure of tyrosinase and peptide docking. (**a**) The active site of tyrosinase, with *p*-tyrosol (green) in the active site (PDB code: 4P6T). The binding modes of native peptide (**b**) and palm-peptide (**c**) in the active site of tyrosinase.

In light of the docking results of tyrosine, we performed the docking studies of native peptide and palm-peptide with tyrosinase. The result showed that the hydroxyl group (red part) in native peptide and palm-peptide was directed toward CuA at a distance of 3.1 Å and 3.2 Å, respectively, and the benzyl ring (green part) also formed a π–π interactions with H208, similar to those of tyrosine (Fig. 3b and 3c). The results indicated that the native peptide and the palm-peptide exhibited similar biological activity towards tyrosinase.

3.2. Physicochemical properties of the peptides

The palm-peptide was derived from its parent compound, namely, the native peptide, to reduce the formation of zwitterions and increase lipophilicity. For palm-peptide, N-terminal was palmitoylated, C-terminal was modified to amide, and the tyrosine at position 6 was changed from *L*- to *D*- form. After C-terminal esterification, the originally ionizable carboxyl group no longer formed charged ions as seen in palm-peptide. Both peptides have high molecular weight, rendering it difficult for them to permeate the skin. After molecular modification, the resultant palm-peptide showed a higher LogP of −0.8 than the native peptide, which has a LogP of −6.5 (Table 1). The increased lipophilicity may increase the skin retention and permeation of the peptide.

3.3. Peptide modification and physicochemical properties

The peptide structures were verified by using HPLC and mass spectrometry (MS) analysis (Fig. 4). Although palm-peptide's lipophilicity increased after modifications, its retention time was shorter than the native peptide. The reason can be ascribed to the different organic phase ratio in the gradient elution program, i.e., 20% for the native peptide while 40% for the palm-peptide. The higher amount of organic solvent in the mobile phase shortened the retention time of modified peptide, despite the increased lipophilicity. The molecular structure of the peptide was verified by the MS spectra of the $[M + 3H]^{3+}$ in *m/z* 466.25 and $[M + 2H]^{2+}$ in *m/z* 698.95 for native peptide and the $[M + 3H]^{3+}$ in *m/z* 545.40 and $[M + 2H]^{2+}$ in *m/z* 817.60 for palm-peptide.

3.4. In vitro skin permeation of peptides

PG is a commonly used ingredient in cosmetics as a co-solvent and/or skin permeation enhancer. Hence, pure PG and PG containing 5% (w/v) CPEs were also used to prepare peptide solutions.

The time course of both peptides in different drug delivery systems is shown in Fig. 5a. Out of the 10 formulations containing either native peptide or palm-peptide, the highest skin permeation was found to be the palm-peptide in the PG solution containing 5% (w/v) menthol. It was worth noting that native peptides only achieved detectable skin permeation in the MN patch formulation. The skin permeation of native peptide in all 4 PG-based liquid formulations were not detected, hence not shown in Fig. 5.

Besides, the cumulative amounts of peptide at different time points were normalized against the dose (Fig. 5b), in which the native peptide showed the highest percentage ($P < 0.0001$).

It was shown in Fig. 5, that the time course of peptide permeation was different from that of a solution maintained at a constant concentration in the donor compartment, in which case the drug permeation rate gradually increases in the beginning and reaches the steady state after a period of permeation (Kang et al., 2005). As a result, the constant flux was not attained within 24 h and the permeation coefficient varied. Accordingly, the cumulative skin permeation and retention in 24 h were used to characterize and compare peptide permeation through skin, in Fig. 6 **and** Fig. 7, respectively.

3.5. Cumulative peptide permeation in 24 h

The cumulative permeation of the two peptides in 24 h from different carriers is shown in Fig. 6a. For the PG-based liquid formulations, the highest permeation of palm-peptide was found in 5% (w/v) menthol,

Table 1
In silico predication of the physicochemical properties of the peptides.

	Native peptide	Palm-peptide
Sequence	YRSRKYSSWY	YRSRK[*Y]SSWY
Formula	$C_{65}H_{90}N_{18}O_{17}$	$C_{81}H_{121}N_{19}O_{17}$
LogP	−6.5	−0.8
MW (Da)	1395.5	1633.0
H-donors	19	18
H-acceptors	28	29
Solubility (mg/ml)	1000	2.6

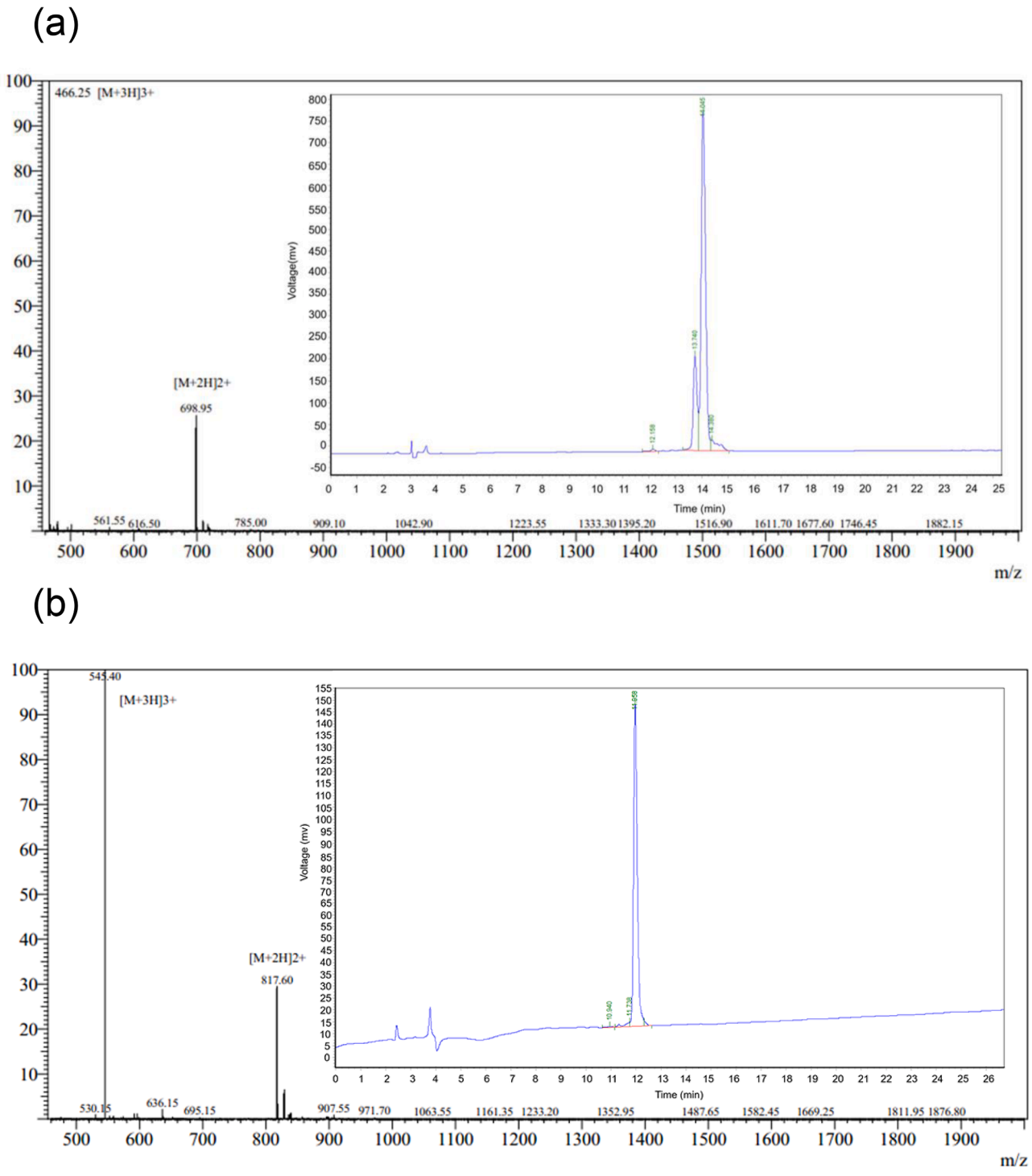

Fig. 4. HPLC and MS data for native peptide (**a**) and palm-peptide (**b**).

which delivered ~ 50 μg palm-peptide through skin in 24 h. For MN patches, a significantly higher amount of native peptide (~40 μg) permeated through the skin than the palm-peptide. All 5 formulations containing the palm-peptide showed detectable skin permeation, while native peptide only showed detectable skin permeation when being formulated inside the MN patch.

After normalization by dose (Fig. 6b), the native peptide permeated ~ 2.5% in 24 h, the highest percentage among all formulations. This indicated that the native peptide in MN patch formulation was the most efficient formulation, in terms of utilization of the drug in the formulation, i.e., the bioavailability in skin.

3.6. Skin retention of the peptides

While skin permeation is the critical step for the peptide to enter skin, its skin retention is also a consideration. The peptide needs to maintain an effective concentation within skin, to act on melanocytes, and reduce the melanin content.

The skin retention of the two peptides after the 24 h *in vitro* skin permeation study is shown in Fig. 7a. Out of the 10 formulations, only 3 formulations, which all contain palm-peptide, showed detectable amounts of palm-peptide in the skin sample. The amount of palm-peptide was less than ~ 0.8 μg per skin sample (skin permeation area

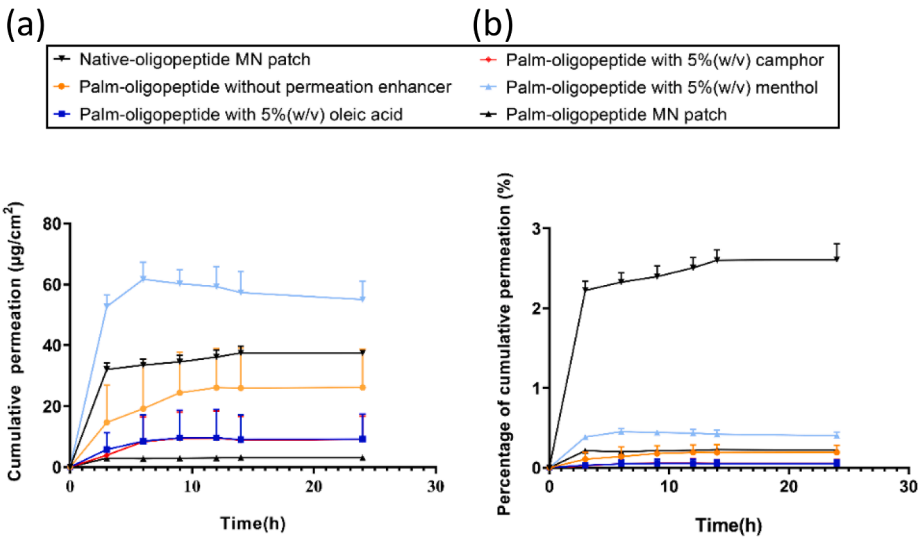

Fig. 5. Cumulative permeation of the peptides over 24 h in different carriers. The native peptide in MN patch and the palm-peptide in MN patch, PG, PG with 5% (w/v) oleic acid, PG with 5% (w/v) camphor, PG with 5% (w/v) menthol: amounts (**a**) and percentage (**b**). The skin permeation of peptide was not detected from all 4 PG-based formulations containing the native peptide.

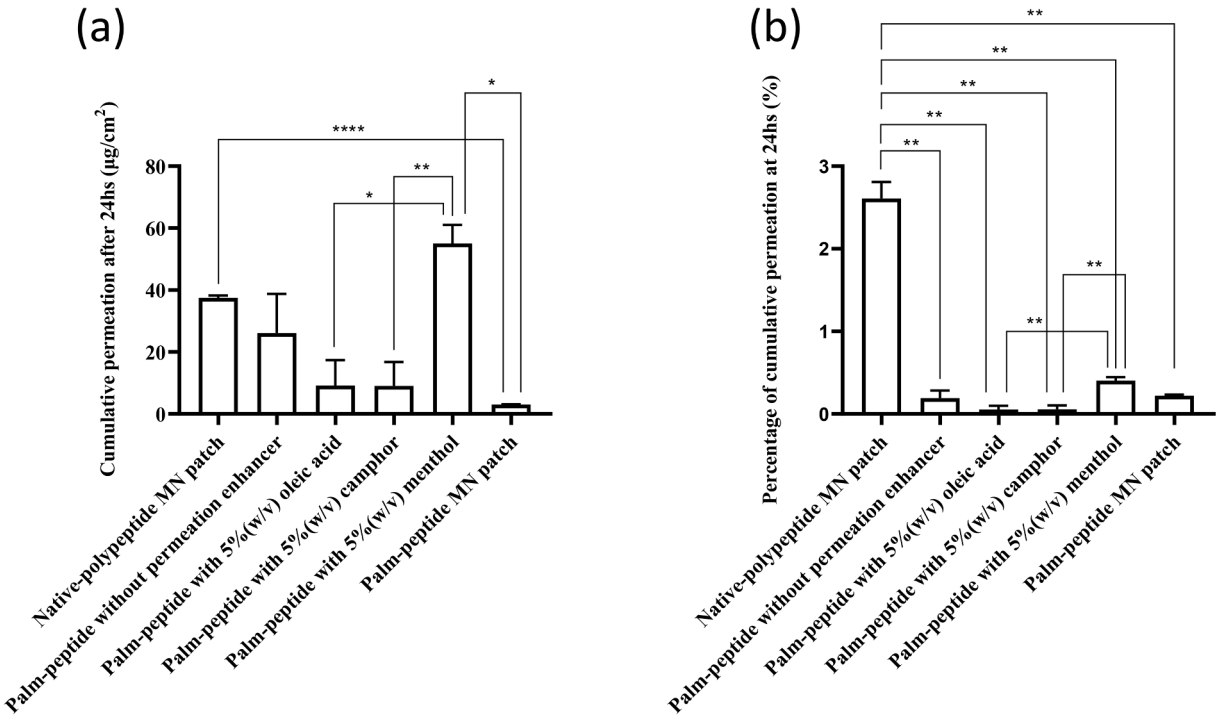

Fig. 6. Cumulative amount of peptide permeated through skin after 24 h, in amounts (**a**) and percentage (**b**). (*, $P < 0.05$; **, $P < 0.01$; ***, $P < 0.001$; ****, $P < 0.0001$). The skin permeation of peptide was not detected from all 4 PG-based formulations containing the native peptide.

$= 1.327\ cm^2$). For the other 7 formulations, no peptide was detected in the skin samples.

After dose normalization (Fig. 7b), it was found that the percentage of palm-peptide retained in the skin when using MN patch was significantly higher than the other two PG-based liquid formulations, showing that MN patch enhanced the partition of the palm-peptide into skin.

4. Discussion

4.1. Skin permeation of the peptides

The outermost lipophilic layer of the skin, namely, SC, is the major obstacle to transcutaneous penetration of therapeutic agents. This lipophilic layer ensures that only small and moderately lipophilic molecules can traverse the skin in sufficient quantities to elicit therapeutically relevant effects (Ita, 2014).

For topical formulations, IVPT can be used to evaluate the cutaneous absorption of a drug. It has been shown that transcutaneous absorption data obtained from the excised human skin model closely approximate those obtained from living man (Lehman et al., 2011). Recently, the US FDA published several product-specific guidances, which allow clinical-trial waiver, by requesting IVPT as part of the study to show bioequivalence between generic and the reference products (Dandamudi, 2017; FDA, 2020).

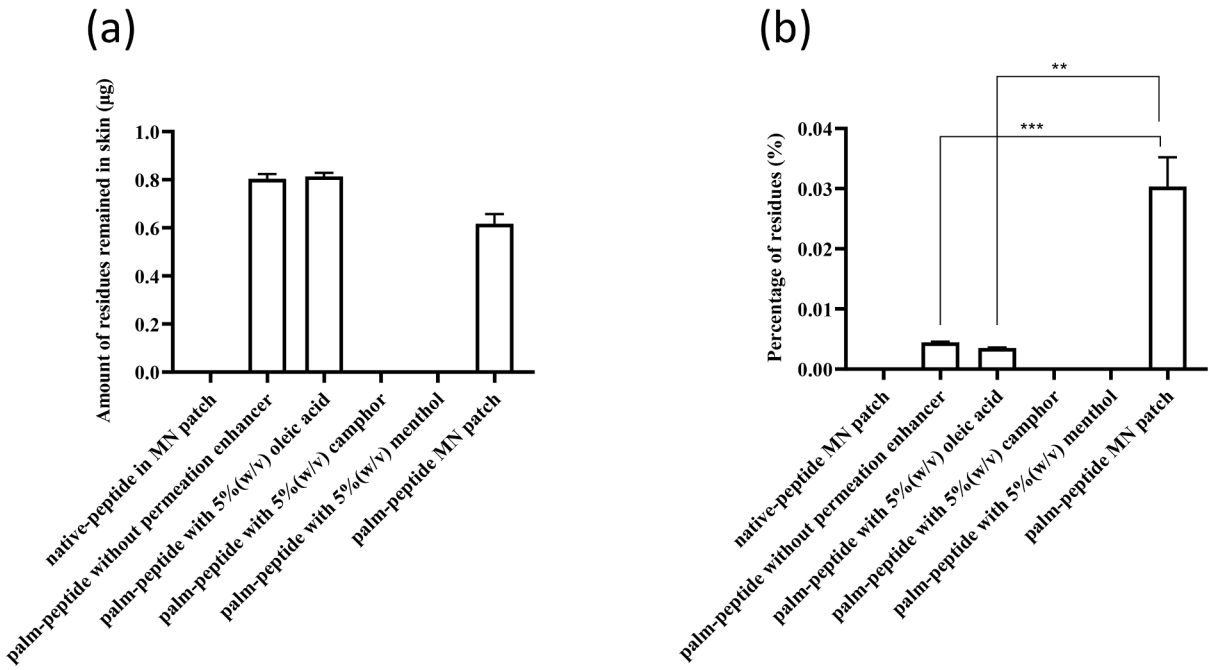

Fig. 7. Skin retention of two peptides in each skin sample, after 24 h of skin permeation testing, in amounts (**a**) and percentage (**b**). Out of the 10 formulations, only 3 formulation showed skin retention of the peptides. (**, $P < 0.01$; ***, $P < 0.001$).

Peptides with large molecular weight and hydrophilic properties cannot penetrate SC in sufficient amounts. Hence, we modified the termini of the native peptide and synthesized the palm-peptide. Because of the higher lipophilicity of palm-peptide than native peptide, there was a corresponding increase in the amount of permeation in 24 h (Fig. 6a) in PG solutions. This suggested the feasibility of chemical modification in promoting transdermal delivery of peptides using PG solution.

4.2. Skin retention of the peptides

Since the two peptides target melanocytes to exert their therapeutic effect (Abu Ubeid et al., 2009), and melanocytes are located in the basal layer of the epidermis, we assessed the peptides' retention inside skin. In comparison to undetectable skin retention of native peptide using 5 formulations containing native peptide, there was apparent skin retention of palm-peptide, as shown by 3 of the 5 formulations containing palm-peptide (Fig. 7a). The increased skin retention of the peptide can be ascribed to its increased lipophilicity because of palmitoylation. Therefore, structural modification of native peptide can potentially increase its efficacy topically by increasing its skin retention.

4.3. The effect of CPEs on skin permeation of the peptides

CPEs can enhance transdermal delivery for various molecules (Ibrahim and Li, 2010; Monti et al., 2001). One mechanism of action has been described as the 'pull-push' effect (Haque and Talukder, 2018). The difference between CPE and the drug, in terms of affinity, would push the drug molecules through SC. Considering the hydrophilic nature of both peptides (Table 1), oleic acid, camphor, and menthol were selected, as they were lipophilic, hence have low affinity towards the peptides. (Table 2). Based on the theory, we expected that oleic acid would exhibit the best enhancement, due to the greater LogP difference between the peptide and oleic acid, than that between the peptide and camphor/menthol. However, the result showed otherwise (Fig. 6a).

Table 2
The properties of three chemical penetration enhancers.

	Oleic acid	Camphor	Menthol
LogP	7.4 ± 0.2	2.1 ± 0.3	3.2 ± 0.2
MW (Da)	282.5	152.2	156.3
Solubility (mg/ml)	0.002	1.1	1.5

For the native peptide, the 3 CPEs did not enhance its skin permeation to a detectable level. For the palm-peptide, none of the 3 CPEs showed significant enhancing effect, as compared to the pure PG solution. On the other hand, however, the PG solution containing 5% menthol delivered significantly higher amounts of palm-peptide than the PG solution containing either 5% camphor or 5% oleic acid.

For menthol and camphor, the result was consistent with our previous findings, that terpene CPEs with higher lipophilicity had better enhancing effect, as menthol has higher LogP values than camphor (Kang et al., 2007).

For menthol and oleic acid, the enhancement mechanism of menthol was reported to be the disruption of the highly ordered SC lipids and improving partition of drugs into SC lipids (Yang et al., 2016). In comparison, oleic acids cause SC lipid phase separation and form a permeable liquid domain inside SC intercellular lipids (Mak et al., 1990). For the palm-peptide, menthol exhibited greater enhancement than the oleic acid, which may be because menthol improved its partition into SC lipids, while the liquid lipid domain induced by oleic acid did not enhance the transport of the hydrophilic molecule, even after molecular modification.

4.4. The effect of MNs on skin permeation of peptides

In this study, both peptides were encapsulated into menthol-based MN patches, which can melt and/or dissolve, upon contact with skin. Interestingly, menthol is also a CPE, which showed enhancing effect on the palm-peptide, in PG solution. Compared with the menthol MN patch, 5% w/v menthol in PG showed greater enhancing effect (Fig. 6a), showing the synergist effect of menthol and PG outweighed the effect of menthol plus MNs. To our knowledge this is the first time a CPE was used to fabricate MNs.

In the MN patch, the native peptide showed greater skin permeation than the palm-peptide (Fig. 6a). This can be attributed to the higher

solubility of the native peptide in aqueous solution than the palm-peptide (Table 1). MNs can impair the skin barrier by creating micro-scale passages through the skin to facilitate peptide penetration through skin. The native peptide, as a macromolecule with high polarity, tends to diffuse into the receptor PBS solution, in which the native peptide is miscible. The palm-peptide, on the other hand, tends to stay with the lipophilic SC layer, with its increased lipophilicity (Fig. 7a).

It was noted that MN patch was the only formulation that resulted in skin permeation of the native peptide, showing the possibility of using the native peptide. However, the disadvantages are as follows. First, the MN patch did not enhance the skin retention of the native peptide. Second, the manufacturing of MN patches is technically demanding.

4.5. Estimation of palm-peptide concentration inside the skin

Based on the skin retention result after application of the palm-peptide for 24 h in the PG-based liquid formulations (Fig. 7a) and the weight of dermatomed skin specimen used in the *in vitro* skin permeation study, the palm-peptide concentration in the skin samples was estimated to be ~ 6 μM (~9 μg in 1 g of the skin sample), which was comparable to the effective concentration (10 μM) and much lower than the toxic concentration (100 μM) (Abu Ubeid et al., 2009).

It should be noted, however, the estimation was based on the assumption that the palm-peptide exhibits similar biological function as the native peptide, as shown by our *insilico* docking result (Fig. 3). To this end, further investigation is warranted to confirm the efficacy and toxicity of the palm-peptide using cellular and/or animal models.

5. Conclusion

In this study, we used molecular modification, CPEs, and MN patches to improve peptide skin permeation and retention. Palmitoylation of the native peptide increased its skin retention and permeation in PG-based liquid formulations. CPEs exhibited a positive effect on skin permeation of the palm-peptide but no effect on the native peptide. Therefore, for the peptide to target melanocytes located in the epidermal basal layer, structural modifications which increase lipophilicity, and CPEs which enhance skin permeability, can be used in combination to achieve the optimal effect.

CRediT authorship contribution statement

Jungen Chen: Methodology, Investigation, Writing - original draft. **Junxing Bian:** Methodology, Investigation, Writing - original draft. **Basil M. Hantash:** Methodology, Writing - review & editing. **Lamyaa Albakr:** Writing - review & editing. **David E. Hibbs:** Software. **Xiaoqiang Xiang:** Software. **Peng Xie:** Software. **Chunyong Wu:** Methodology, Investigation, Supervision, Writing - review & editing. **Lifeng Kang:** Conceptualization, Methodology, Writing - review & editing, Supervision, Funding acquisition, Project administration.

Declaration of Competing Interest

The authors declare that they have no known competing financial interests or personal relationships that could have appeared to influence the work reported in this paper.

Acknowledgment

The authors acknowledge the support from the University of Sydney. The research also received funding support from Escape Therapeutics Inc., USA, and the National Natural Science Foundation of China (No. 82074128).

Appendix A. Supplementary data

Supplementary data to this article can be found online at https://doi.org/10.1016/j.ijpharm.2021.120868.

References

Abu Ubeid, A., Zhao, L., Wang, Y., Hantash, B.M., 2009. Short-sequence oligopeptides with inhibitory activity against mushroom and human tyrosinase. J Invest Dermatol 129, 2242–2249.
Ahad, A., Aqil, M., Kohli, K., Chaudhary, H., Sultana, Y., Mujeeb, M., Talegaonkar, S., 2009. Chemical penetration enhancers: a patent review. Expert Opin Ther Pat 19, 969–988.
Antosova, Z., Mackova, M., Kral, V., Macek, T., 2009. Therapeutic application of peptides and proteins: parenteral forever? Trends Biotechnol 27, 628–635.
Bhatia, A., Hsu, J., Hantash, B.M., 2014. Combined topical delivery and dermalinfusion of decapeptide-12 accelerates resolution of post-inflammatory hyperpigmentation in skin of color. J Drugs Dermatol 13, 84.
Cichorek, M., Wachulska, M., Stasiewicz, A., Tyminska, A., 2013. Skin melanocytes: biology and development. Postepy Dermatol Alergol 30, 30–41.
Costello, C.T., Jeske, A.H., 1995. Iontophoresis: applications in transdermal medication delivery. Phys Ther 75, 554–563.
Dandamudi, S., 2017. In vitro bioequivalence data for a topical product: bioequivalence review perspective. FDA Public Workshop.
FDA, 2020. Product-specific guidances for generic drug development https://www.fda.gov/drugs/guidances-drugs/product-specific-guidances-generic-drug-development.
Goldfeder, M., Kanteev, M., Isaschar-Ovdat, S., Adir, N., Fishman, A., 2014. Determination of tyrosinase substrate-binding modes reveals mechanistic differences between type-3 copper proteins. Nat Commun 5, 4505.
Gómez, C., Benito, M., Teijón, J.M., Blanco, M.D., 2012. Novel methods and devices to enhance transdermal drug delivery: the importance of laser radiation in transdermal drug delivery. Ther Deliv 3, 373–388.
Hantash, B.M., 2018. Enhanced topical uptake of ascorbic acid in fractional photothermolysis-treated ex vivo human skin. J Dermatol Surg Res Ther 2018, 20–27.
Hantash, B.M., Jimenez, F., 2009. A split-face, double-blind, randomized and placebo-controlled pilot evaluation of a novel oligopeptide for the treatment of recalcitrant melasma. J Drugs Dermatol 8, 732–735.
Hantash, B.M., Jimenez, F., 2012. Treatment of mild to moderate facial melasma with the Lumixyl topical brightening system. J Drugs Dermatol 11, 660–662.
Haque, T., Talukder, M.M.U., 2018. Chemical enhancer: a simplistic way to modulate barrier function of the stratum corneum. Adv Pharm Bull 8, 169–179.
Ibrahim, S.A., Li, S.K., 2010. Efficiency of fatty acids as chemical penetration enhancers: mechanisms and structure enhancement relationship. Pharm Res 27, 115.
Ita, K., 2014. Transdermal drug delivery: progress and challenges. J Drug Deliv Sci Technol 24, 245–250.
Kang, L., Ho, P.C., Chan, S.Y., 2006. Interactions between a skin penetration enhancer and the main components of human stratum corneum lipids - Isothermal titration calorimetry study. J Therm Anal Calorim 83, 27–30.
Kang, L., Liu, X.Y., Sawant, P.D., Ho, P.C., Chan, Y.W., Chan, S.Y., 2005. SMGA gels for the skin permeation of haloperidol. J Control Release 106, 88–98.
Kang, L., Yap, C.W., Lim, P.F., Chen, Y.Z., Ho, P.C., Chan, Y.W., Wong, G.P., Chan, S.Y., 2007. Formulation development of transdermal dosage forms: quantitative structure-activity relationship model for predicting activities of terpenes that enhance drug penetration through human skin. J Control Release 120, 211–219.
Kathuria, H., Kang, K., Cai, J., Kang, L., 2020. Rapid microneedle fabrication by heating and photolithography. Int J Pharm 575, 118992.
Kathuria, H., Li, H., Pan, J., Lim, S.H., Kochhar, J.S., Wu, C., Kang, L., 2016. Large size microneedle patch to deliver lidocaine through skin. Pharm Res 33, 2653–2667.
Koh, K.J., Liu, Y., Lim, S.H., Loh, X.J., Kang, L., Lim, C.Y., Phua, K.K.L., 2018. Formulation, characterization and evaluation of mRNA-loaded dissolvable polymeric microneedles (RNApatch). Sci Rep 8, 11842.
Kumar, R., Philip, A., 2007. Modified transdermal technologies: Breaking the barriers of drug permeation via the skin. Trop J Pharm Res 6, 633–644.
Lehman, P.A., Raney, S.G., Franz, T.J., 2011. Percutaneous absorption in man: in vitro-in vivo correlation. Skin Pharmacol Physiol 24, 224–230.
Li, H., Low, Y.S.J., Chong, H.P., Zin, M.T., Lee, C.-Y., Li, B., Leolukman, M., Kang, L., 2015. Microneedle-mediated delivery of copper peptide through skin. Pharm Res 32, 2678–2689.
Lim, S.H., Sun, Y., Thiruvallur Madanagopal, T., Rosa, V., Kang, L., 2018. Enhanced skin permeation of anti-wrinkle peptides via molecular modification. Sci Rep 8, 1596.
Lim, S.H., Tiew, W.J., Zhang, J., Ho, P.C., Kachouie, N.N., Kang, L., 2020. Geometrical optimisation of a personalised microneedle eye patch for transdermal delivery of anti-wrinkle small peptide. Biofabrication 12, 035003.
Lombry, C., Dujardin, N., Préat, V., 2000. Transdermal delivery of macromolecules using skin electroporation. Pharm Res 17, 32–37.
Ma, G., Wu, C., 2017. Microneedle, bio-microneedle and bio-inspired microneedle: A review. J Control Release 251, 11–23.
Mak, V.H., Potts, R.O., Guy, R.H., 1990. Percutaneous penetration enhancement in vivo measured by attenuated total reflectance infrared spectroscopy. Pharm Res 7, 835–841.
Mitragotri, S., Blankschtein, D., Langer, R., 1995. Ultrasound-mediated transdermal protein delivery. Science 269, 850–853.

Monti, D., Giannelli, R., Chetoni, P., Burgalassi, S., 2001. Comparison of the effect of ultrasound and of chemical enhancers on transdermal permeation of caffeine and morphine through hairless mouse skin in vitro. Int J Pharm 229, 131–137.
Morimoto, Y., Wada, Y., Seki, T., Sugibayashi, K., 2002. In vitro skin permeation of morphine hydrochloride during the finite application of penetration-enhancing system containing water, ethanol and l-menthol. Bio Pharm Bull 25, 134–136.
Parvez, S., Kang, M., Chung, H.S., Cho, C., Hong, M.C., Shin, M.K., Bae, H., 2006. Survey and mechanism of skin depigmenting and lightening agents. Phytother Res 20, 921–934.
Pierre, M.B., Ricci Jr., E., Tedesco, A.C., Bentley, M.V., 2006. Oleic acid as optimizer of the skin delivery of 5-aminolevulinic acid in photodynamic therapy. Pharm Res 23, 360–366.
Prausnitz, M.R., 2004. Microneedles for transdermal drug delivery. Adv Drug Deliv Rev 56, 581–587.
Schuetz, Y.B., Naik, A., Guy, R.H., Kalia, Y.N., 2005. Emerging strategies for the transdermal delivery of peptide and protein drugs. Expert Opin Drug Deliv 2, 533–548.
Torok, H.M., 2006. A comprehensive review of the long-term and short-term treatment of melasma with a triple combination cream. Am J Clin Dermatol 7, 223–230.
Williams, A.C., Barry, B.W., 2012. Penetration enhancers. Adv Drug Del Rev 64, 128–137.
Xie, F., Chai, J.K., Hu, Q., Yu, Y.H., Ma, L., Liu, L.Y., Zhang, X.L., Li, B.L., Zhang, D.H., 2016. Transdermal permeation of drugs with differing lipophilicity: Effect of penetration enhancer camphor. Int J Pharm 507, 90–101.
Yang, S., Wang, R., Wan, G., Wu, Z., Guo, S., Dai, X., Shi, X., Qiao, Y., 2016. A multiscale study on the penetration enhancement mechanism of menthol to osthole. J Chem Inf Model 56, 2234–2242.